Yap/Taz mediates mTORC2-stimulated fibroblast activation and kidney fibrosis

Received for publication, May 20, 2018, and in revised form, August 7, 2018 Published, Papers in Press, August 28, 2018, DOI 10.1074/jbc.RA118.004073

Yuan Gui[1], **Jianzhong Li**[1], **Qingmiao Lu, Ye Feng, Mingjie Wang, Weichun He, Junwei Yang, and Chunsun Dai**[2]

From the Center for Kidney Disease, Second Affiliated Hospital, Nanjing Medical University, 262 North Zhongshan Road, Nanjing, Jiangsu 210003, China

Edited by Alex Toker

Our previously published study demonstrated that mammalian target of rapamycin complex 2 (mTORC2) signaling mediates TGFβ1-induced fibroblast activation. However, the underlying mechanisms for mTORC2 in stimulating fibroblast activation remain poorly understood. Here, we found that TGFβ1 could stimulate mTORC2 and Yap/Taz activation in NRK-49F cells. Blocking either mTORC2 or Yap/Taz signaling diminished TGFβ1-induced fibroblast activation. In addition, blockade of mTORC2 could down-regulate the expression of Yap/Taz, connective tissue growth factor (*CTGF*), and ankyrin repeat domain 1 (*ANKRD1*). Overexpression of constitutively active Taz (Taz-S89A) could restore fibroblast activation suppressed by PP242, an mTOR kinase inhibitor in NRK-49F cells. In mouse kidneys with unilateral ureter obstructive (UUO) nephropathy, both mTORC2 and Yap/Taz were activated in the interstitial myofibroblasts. Ablation of Rictor in fibroblasts/pericytes or blockade of mTOR signaling with PP242 attenuated Yap/Taz activation and UUO nephropathy in mice. Together, this study uncovers that targeting mTORC2 retards fibroblast activation and kidney fibrosis through suppressing Yap/Taz activation.

Chronic kidney disease, pathologically manifested as interstitial excessive extracellular matrix (ECM)[3] deposition and kidney fibrosis, is a leading cause for end-stage renal failure (1, 2). Among all of the cell types, fibroblast is the major source for interstitial ECM production (3–5). To date, the mechanisms regulating fibroblast activation and kidney fibrosis remain to be further determined.

This work was supported by National Science Foundation of China Grants 81570611/H0503 and 81770675/H0503 (to D. C.) and 81700589 (to J. L.) and Science Foundation of Jiangsu Province Grant BK20140048 (to D. C.). The authors declare that they have no conflicts of interest with the contents of this article.

This article contains Figs. S1 and S2.

[1] Both authors contributed equally to this work.

[2] To whom correspondence should be addressed. Tel.: 86-25-52636077; E-mail: daichunsun@njmu.edu.cn.

[3] The abbreviations used are: ECM, extracellular matrix; Yap, Yes-associated protein; Taz, transcriptional co-activator with PDZ-binding motif; mTOR, mammalian target of rapamycin; mTORC, mammalian target of rapamycin complex; UUO, unilateral ureter obstruction; CTGF, connective tissue growth factor; ANKRD1, ankyrin repeat domain 1; TEAD, TEA domain; CHX, cycloheximide; p-, phosphorylated; DAPI, 4′,6-diamidino-2-phenylindole; TGF, transforming growth factor; GAPDH, glyceraldehyde-3-phosphate dehydrogenase; SMA, smooth-muscle actin; FN, fibronectin.

The Hippo pathway is an evolutionarily conserved kinase cascade that exerts crucial effects on regulating cell proliferation, organ size, and tissue regeneration (6). The core components of the Hippo pathway include Mst1/2, Sav1, Lats1/2, MOB1A, MOB1B, Yes-associated protein (Yap), and its paralogue transcriptional co-activator with PDZ-binding motif (Taz). Among them, Yap and Taz, classically activated by reducing Hippo pathway–mediated phosphorylation under certain stimuli, exhibit overlapping functions when expressed in the same cell (6–9). After translocation into the nucleus, Yap/Taz interacts with several transcription factors, such as the TEA domain (TEAD) transcription factor family (TEAD1–4), ErbB4, and p73 to regulate target gene expression (10, 11). In addition to the classic Hippo pathway, Yap/Taz may also be regulated by the Hippo-independent pathways (12, 13). In diabetic nephropathy, activation of the EGFR-PI3K-Akt-CREB signaling pathway may up-regulate the expression of Yap and its target genes, including connective tissue growth factor (*CTGF*) and amphiregulin (14). Recently, Yap/Taz has been reported to be able to stimulate fibroblast activation and kidney fibrosis (15, 16). However, the mechanisms for regulating Yap/Taz activity during fibroblast activation and kidney fibrosis are not fully clarified.

The mammalian target of rapamycin (mTOR), an evolutionarily conserved member of the phosphatidylinositol-3-OH -kinase–related kinase family, plays an essential role in regulating cell growth, proliferation, and survival. As a core component, mTOR participates in forming two distinct complexes, named mTOR complex 1 (mTORC1) and mTOR complex 2 (mTORC2) (17, 18). MTORC2, composed of mTOR, Rictor, mSIN1, Protor-1, mLST8, and Deptor, plays a key role in modulating cell survival, metabolism, proliferation, and cytoskeleton homeostasis (19–23). Our previously published study (24) demonstrated that mTORC2 signaling stimulates fibroblast activation and kidney fibrosis. Recently, accumulated evidence has unveiled interactions between mTORC2 and Hippo pathways. Sciarretta *et al.* (25) reported that Rictor/mTORC2 restrains the activity of MST1 kinase to preserve cardiac structure and function. Artinian *et al.* (26) found that mTORC2 can up-regulate the expression of Yap target genes through phosphorylating AMOTL2 at the site of Ser-760. Thus, we predicated that Rictor/mTORC2 may promote fibroblast activation and kidney fibrosis through stimulating Yap/Taz activation.

Here, we report that Rictor/mTORC2 signaling mediated TGFβ1-stimulated Yap/Taz up-regulation in kidney fibro-

blasts. Blockade of mTORC2 signaling could largely reduce Yap/Taz activation and kidney fibrosis in mice with unilateral ureter obstructive (UUO) nephropathy.

Results

Blockade of Rictor/mTORC2 signaling attenuates TGFβ1-induced Yap/Taz up-regulation

To investigate the role for mTORC2 signaling in Yap/Taz activation in kidney fibroblasts, we generated primary cultured mouse kidney fibroblasts from Rictor$^{fl/fl}$ mice and infected the cells with adenovirus carrying Cre recombinase for 48 h to induce *Rictor* gene deletion (Fig. S1). The fibroblasts were stimulated with TGFβ1 (2 ng/ml) for different durations as indicated. A Western blot assay revealed that TGFβ1 could remarkably up-regulate Yap/Taz expression in a time-dependent manner in the control fibroblasts, whereas ablation of *Rictor* largely prohibited their induction (Fig. 1*A*). We also treated NRK-49F cells, a rat kidney interstitial fibroblast cell line, with the mTOR inhibitor PP242 and mTORC1 inhibitor rapamycin, respectively. The results showed that PP242 at 16 nM could reduce TGFβ1-induced Akt and S6 phosphorylation by about 34 and 39%, respectively (Fig. 1*B*). PP242 but not rapamycin could markedly inhibit TGFβ1-induced Yap/Taz up-regulation (Fig. 1*C*). PP242 treatment could also decrease the mRNA abundance for *Yap*/*Taz* as well as its target genes, including *CTGF* and ankyrin repeat domain 1 (*ANKRD1*), in NRK-49F cells (Fig. 1*D*), whereas rapamycin could not (Fig. 1*E*). The results suggest that mTORC2 is required for TGFβ1-induced Yap/Taz activation in NRK-49F cells.

To further decipher the role of Akt, the major downstream molecule for mTORC2 signaling, in regulating Yap/Taz activity, we treated NRK-49F cells with Akt1/2 inhibitor, followed by TGFβ1 treatment. The results showed that blocking Akt could largely reduce the up-regulation of Yap/Taz, *CTGF*, and *ANKRD1*, respectively (Fig. 1, *F* and *G*). We also treated NRK-49F cells with cycloheximide (CHX) and actinomycin D to inhibit gene translational and transcriptional activity, respectively. The Western blot assay showed that CHX and actinomycin D could largely prohibit TGFβ1-induced Yap/Taz up-regulation (Fig. 1, *H* and *I*). Taken together, it may be concluded that Rictor/mTORC2/Akt signaling is required for TGFβ1-induced Yap/Taz activation in kidney fibroblasts.

Yap/Taz induction mediates mTORC2-stimulated kidney fibroblast activation

Our previous study demonstrated that Rictor/mTORC2 signaling mediates TGFβ1-induced fibroblast activation (24). Consistent with that report, we found that ablation of the *Rictor* gene in primary cultured kidney fibroblasts could largely attenuate TGFβ1-induced fibroblast activation (Fig. 2, *A* and *B*). Blockade of mTOR signaling with PP242 could also markedly inhibit TGFβ1-induced FN and α-SMA protein expression in NRK-49F cells (Fig. 2, *C* and *D*). In addition, blocking Yap/Taz with verteporfin markedly inhibited TGFβ1-induced NRK-49F cell activation (Fig. 2, *E* and *F*). The Western blot assay showed that verteporfin could not affect TGFβ1-stimulated Smad3 phosphorylation (Fig. 2*E*, *right*). NRK-49F cells were also transfected with Yap/Taz siRNAs, respectively. The Western blot assay showed that knocking down Yap/Taz expression could inhibit TGFβ1-induced fibroblast activation (Fig. 2, *G–J*). To further decipher the role for Yap/Taz induction in mediating Rictor/mTORC2-stimulated fibroblast activation, we transfected NRK-49F cells with plasmid carrying a constitutively active form of Taz (Taz-S89A) (27) (Fig. 2*K*). The results showed that expression of Taz-S89A could largely restore TGFβ1-induced fibroblast activation, which was suppressed by PP242 treatment (Fig. 2, *L* and *M*). Taken together, these data demonstrated that Yap/Taz induction mediates mTORC2-stimulated kidney fibroblast activation.

Both mTORC2 and Yap/Taz signaling are activated in myofibroblasts from the fibrotic kidneys with UUO nephropathy

The aforementioned data demonstrated that Yap/Taz mediates mTORC2-stimulated fibroblast activation in cultured kidney fibroblasts. To further decipher the interaction between mTORC2 and Yap/Taz signaling in myofibroblasts within the fibrotic kidneys, we generated UUO model and examined the abundance of these two signaling pathway proteins in the fibrotic kidneys in mice. Pronounced induction of p-Akt (Ser-473), p-Yap (Ser-127), Yap/Taz, and TEAD as well as the reduction of LATS1 were detected in the kidneys at days 3, 7, and 14 after UUO (Fig. 3*A*). The mRNA abundance for *Yap*/*Taz*, *TEAD1–4*, *CTGF*, and *ANKRD1* was increased in the UUO kidneys (Fig. 3*B*). To explore whether both mTORC2 and Yap/Taz were activated in myofibroblasts from the UUO kidneys, we co-stained the UUO kidney tissue with antibodies against α-SMA and p-Akt (Ser-473), Yap/Taz, and TEAD, respectively. The results showed that p-Akt (Ser-473), Yap/Taz, and TEAD could be detected in myofibroblasts from the UUO kidneys. It is of note that p-Akt (Ser-473), Yap/Taz and TEAD were also detected in epithelial cells after UUO (Fig. 3*C*). Together, these data showed that mTORC2 and Yap/Taz are co-activated in the myofibroblasts from the fibrotic kidneys in mice with UUO nephropathy.

Ablation of Rictor in fibroblasts diminishes Yap/Taz activation and UUO nephropathy in mice

To further investigate the role of Rictor/mTORC2 signaling in regulating Yap/Taz and fibroblast activation, we generated a mouse model with inducible ablation of *Rictor* in fibroblast by breeding Rictor-floxed mice with Gli1-CreERT2 transgenic mice (28–30). After breeding several times (Fig. S2*A*), we obtained mice with genotyping Gli1-Cre$^{+/-}$, Rictor$^{fl/fl}$ (Fig. S2*B*, *lane 3*). Mice with genotyping Gli1-Cre$^{+/-}$, Rictor$^{fl/fl}$ were injected intraperitoneally with tamoxifen for 5 consecutive days. The same-sex littermates with genotyping Gli1-Cre$^{-/-}$, Rictor$^{fl/fl}$ were injected with tamoxifen and treated as control littermates. Two days after the last injection, both control littermates and knockouts were subjected to UUO (Fig. 2*C*). The protein abundance for Yap/Taz, FN, and α-SMA was remarkably increased in the UUO kidneys from control littermates compared with the sham kidneys, which was largely decreased in the UUO kidneys from the knockouts (Fig. 4, *A* and *B*). Immune staining further confirmed the reduction of Yap/Taz in myofibroblasts from the knockouts after UUO compared

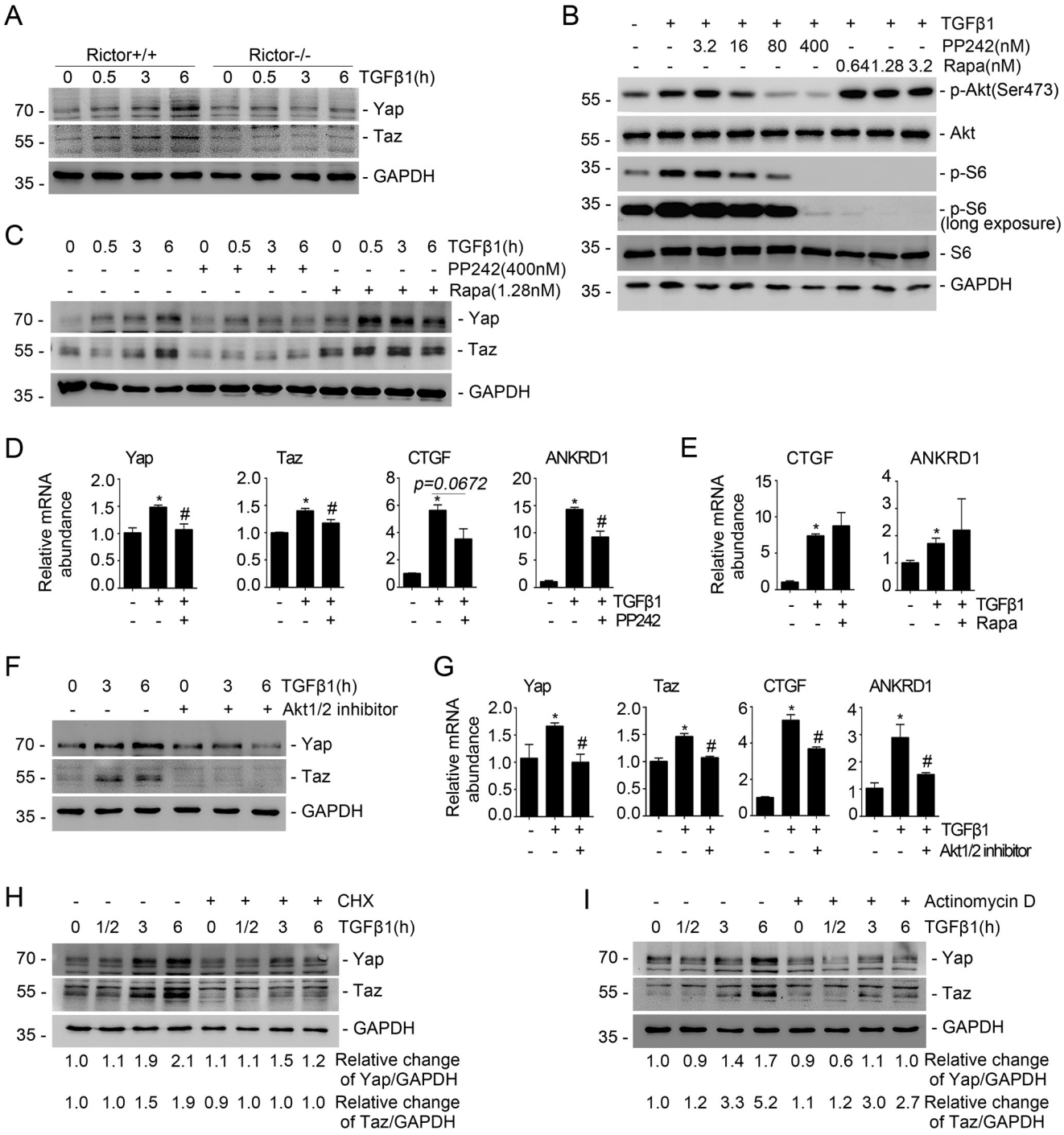

Figure 1. Blockade of Rictor/mTORC2 signaling reduces TGFβ1-induced Yap/Taz expression. *A*, the primary cultured fibroblasts generated from the kidneys of Rictor$^{fl/fl}$ mice were infected with adeno-Cre virus. After 48 h, the fibroblasts were serum-starved overnight and then treated with TGFβ1 (2 ng/ml). Western blot assays show the abundance for Yap/Taz. GAPDH was probed to show the equal loading of the samples. *B*, Western blot analyses showing the abundance of p-Akt (Ser-473) and p-S6 in NRK-49F cells after PP242 or rapamycin treatment. *C*, NRK-49F cells were pretreated with PP242 (400 nM) and rapamycin (1.28 nM) for 30 min, followed by TGFβ1 (2 ng/ml) administration for different durations. The Western blot assay demonstrated that PP242 but not rapamycin could inhibit TGFβ1-induced Yap/Taz expression. *D*, real-time PCR analysis showing the mRNA abundance for *Yap*, *Taz*, *CTGF*, and *ANKRD1* in NRK-49F cells. *, $p < 0.05$ compared with control cells ($n = 3–4$); #, $p < 0.05$ compared with cells treated with TGFβ1 ($n = 3–4$). *E*, real-time PCR analysis showing the mRNA abundance for *CTGF* and *ANKRD1* in NRK-49F cells. *, $p < 0.05$ compared with control cells ($n = 3$). *F*, Western blot analysis showing that Akt1/2 inhibitor could suppress TGFβ1-induced Yap and Taz expression. *G*, real-time PCR analysis showing the mRNA abundance for *Yap*, *Taz*, *CTGF*, and *ANKRD1* in NRK-49F cells. *, $p < 0.05$ compared with control cells ($n = 3–4$); #, $p < 0.05$ compared with cells treated with TGFβ1 ($n = 3–4$). *H* and *I*, NRK-49F cells were treated with cycloheximide (50 μg/ml) or actinomycin D (0.1 μM), followed by TGFβ1 (2 ng/ml) administration. A Western blot assay shows the abundance for Yap and Taz. GAPDH was probed to show the equal loading of the samples. *Error bars*, S.E.

with those from the control littermates (Fig. 4*C*). The mRNA abundance for *Yap*/*Taz*, *TEAD1–4*, *CTGF*, and *ANKRD* was also decreased in the UUO kidneys from the knockouts compared with control littermates (Fig. 4*D*). These results suggest that ablation of *Rictor* in fibroblasts could reduce Yap/Taz and fibroblast activation in mice with UUO nephropathy.

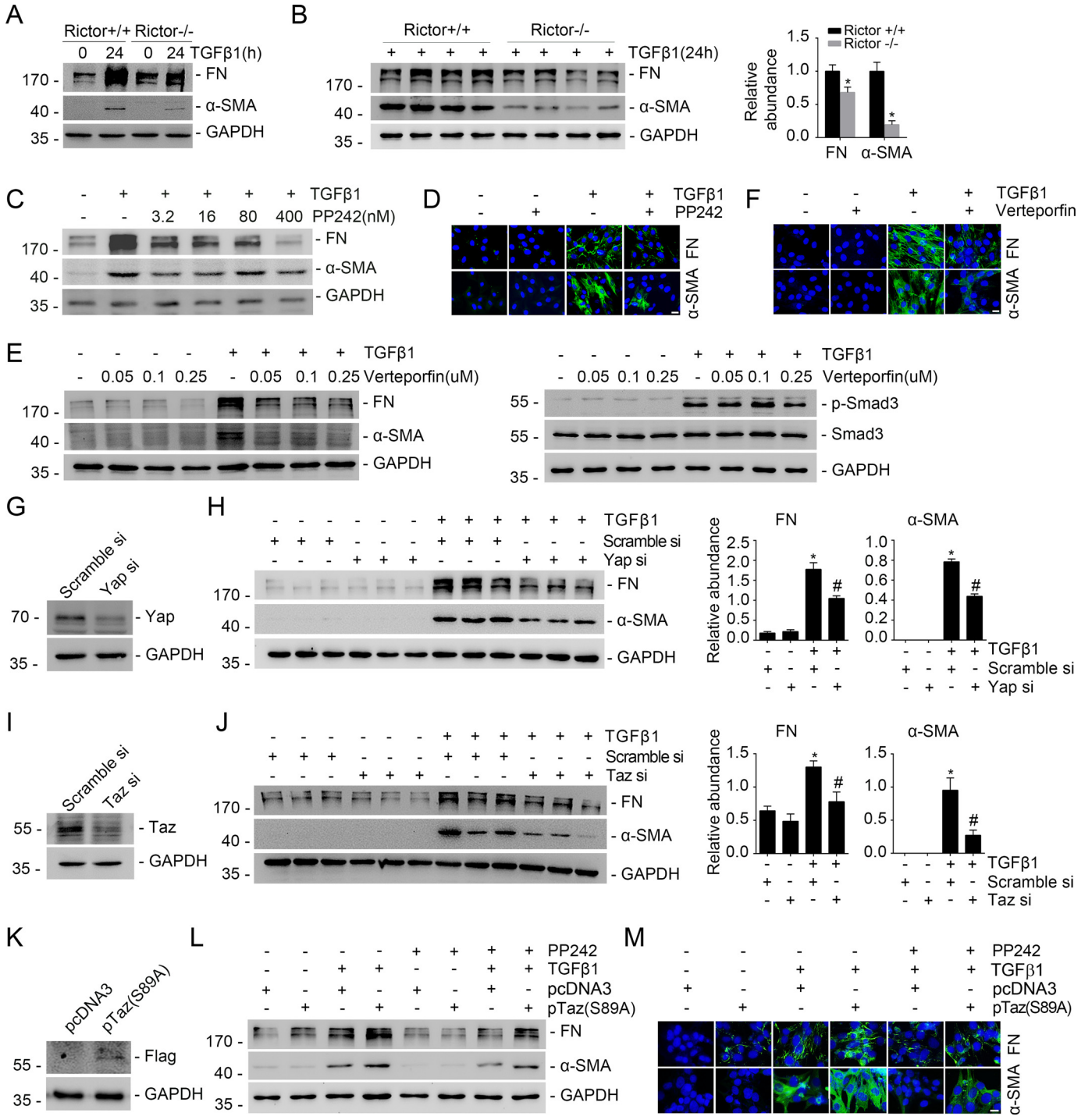

Figure 2. Yap/Taz mediates Rictor/mTORC2-stimulated fibroblast activation. *A*, Western blot assay showing that ablation of *Rictor* reduced TGFβ1-induced FN and α-SMA expression in kidney fibroblasts. *B*, Western blot assay (*left*) and quantitative analysis (*right*) showing the protein abundance for FN and α-SMA in Rictor$^{+/+}$ and Rictor$^{-/-}$ primary cultured kidney fibroblasts. Fibroblasts were treated with TGFβ1 for 24 h. *, $p < 0.05$ compared with Rictor$^{+/+}$ fibroblasts ($n = 4$). GAPDH was probed to show the equal loading of the samples. *C*, Western blot analysis showing that PP242 could dose-dependently inhibit TGFβ1-induced FN and α-SMA expression in NRK-49F cells. *D*, immune staining showing that PP242 could inhibit TGFβ1-induced NRK-49F cell activation. Cells were co-stained with 4′,6-diamidino-2-phenylindole (DAPI) to visualize the nuclei. *Scale bar*, 5 μm. *E*, Western blot analyses showing the abundance of FN and α-SMA expression (*left*) and p-Smad3 (*right*). NRK-49F cells were treated with verteporfin, followed by TGFβ1 administration for 24 h (*left*) or 30 min (*right*). *F*, representative micrographs showing that verteporfin could abolish TGFβ1-induced fibroblast activation in NRK-49F cells. Cells were co-stained with DAPI to visualize the nuclei. *Scale bar*, 5 μm. *G* and *I*, Western blot analyses demonstrating the down-regulation of Yap (*G*) or Taz (*I*) after siRNA transfection, respectively. *H* and *J*, NRK-49F cells were pretreated with scramble, Yap, or Taz siRNA for 24 h, followed by TGFβ1 treatment for 24 h. Western blot analysis shows that knocking down Yap or Taz could reduce TGFβ1-induced FN and α-SMA expression (*left*). *Right*, graphic presentation of FN and α-SMA protein abundance in NRK-49F cells. *, $p < 0.05$ compared with control ($n = 3$); #, $p < 0.05$ compared with TGFβ1-treated cells ($n = 3$). *K* and *L*, Western blot assay showing the expression of exogenous Taz (S89A) in NRK-49F cells after Taz-S89A plasmid transfection (*K*). Western blot assays show the abundance for FN and α-SMA in NRK-49F cells (*L*). NRK-49F cells were transiently transfected with pTaz-S89A, followed 24 h later by TGFβ1 with or without PP242 treatment for 24 h. *M*, representative micrographs showing the immunostaining for FN and α-SMA in fibroblasts after various treatments as indicated. Cells were co-stained with DAPI to visualize the nuclei. *Scale bar*, 5 μm. *Error bars*, S.E.

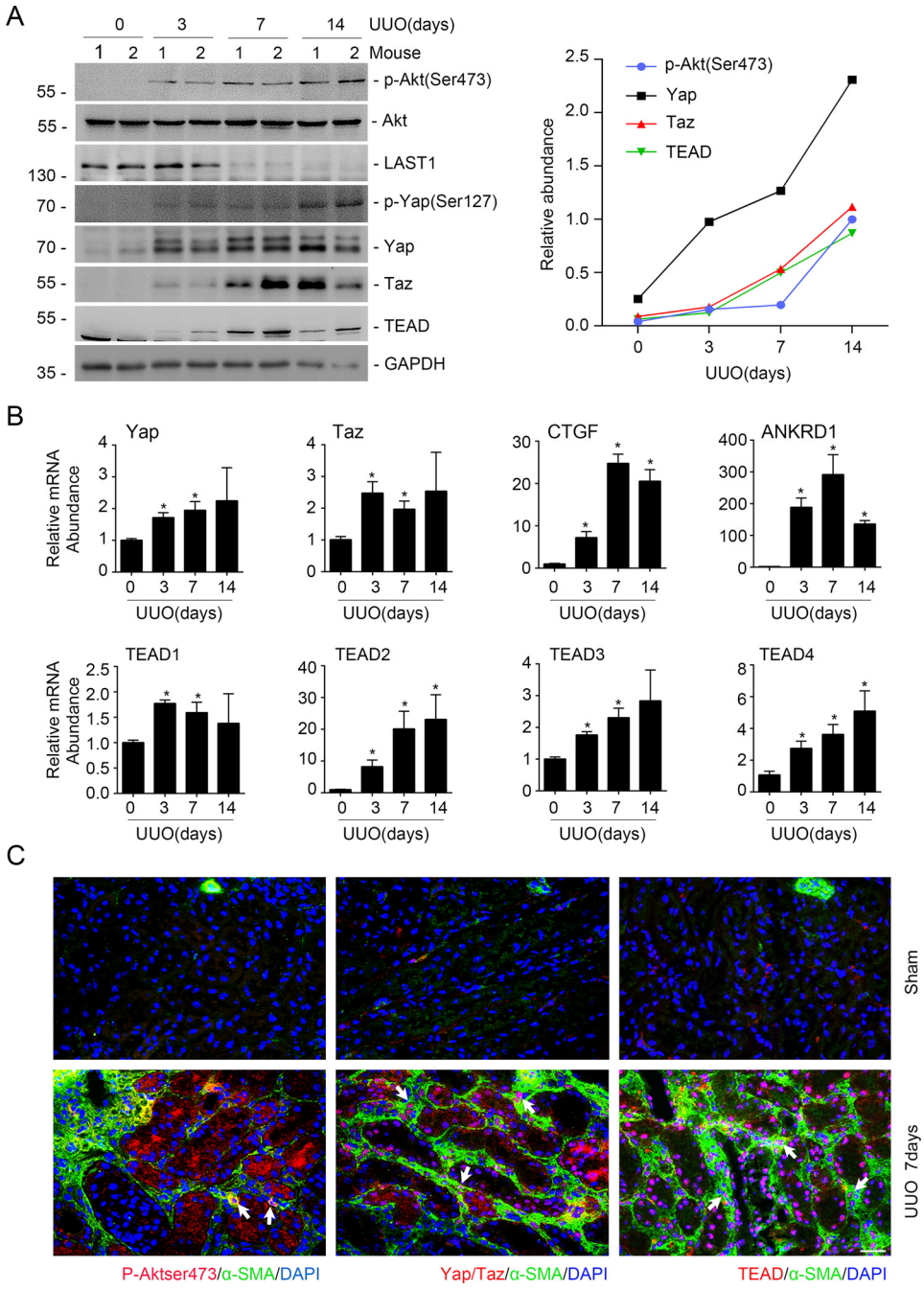

Figure 3. Co-activation of mTORC2 and Yap/Taz signaling in myofibroblasts from the UUO kidneys. *A*, Western blot assay (*left*) and semiquantitative analysis (*right*) showing the induction of p-Akt (Ser-473), p-Yap (Ser-127), Yap, Taz, and TEAD in the UUO kidneys. *B*, real-time RT-PCR analysis showing the mRNA abundance for *Yap*, *Taz*, *CTGF*, *ANKRD1*, and *TEAD1–4* in the UUO kidneys. *, $p < 0.05$ compared with sham control ($n = 3–4$). C, representative images showing the induction for p-Akt (Ser-473), Yap/Taz, and TEAD in myofibroblasts from the UUO kidneys at day 7 after surgery. *White arrows*, myofibroblasts with the induction of p-Akt (Ser-473), Yap/Taz, and TEAD, respectively. *Scale bar*, 20 μm. *Error bars*, S.E.

We stained the kidney sections with periodic acid–Schiff, Masson, and Sirius red. In the UUO kidneys from the control littermates, remarkable tubular atrophy and interstitial extracellular matrix deposition could be detected, which were largely alleviated in the knockout kidneys (Fig. 4*E*). The fibrotic area and total collagen content within the UUO kidneys were also significantly decreased in the knockouts compared with those from the control littermates (Fig. 4, *F* and *G*). Taken together, these data suggest that ablation of *Rictor* in fibroblasts reduces Yap/Taz induction and kidney fibrosis in mice with UUO nephropathy.

Blockade of mTORC2 signaling with PP242 attenuates Yap/Taz induction and UUO nephropathy in mice

In cultured NRK-49F cells, we found that blocking mTORC2 with PP242 could inhibit TGFβ1-induced Yap/Taz signaling activation. We then wanted to know whether PP242 could inhibit Yap/Taz activation and kidney fibrosis in mice with

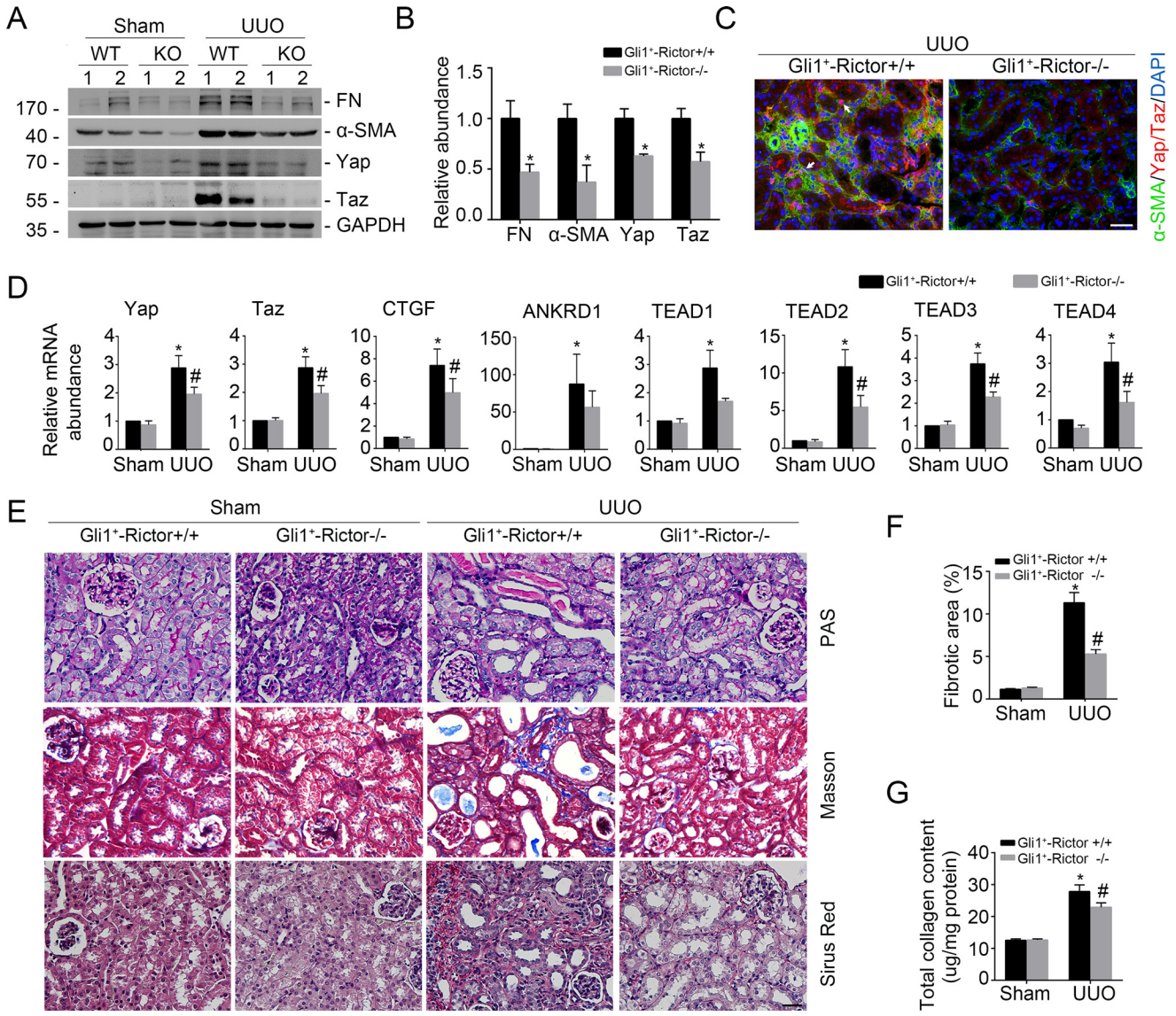

Figure 4. Ablation of Rictor in fibroblasts diminishes Yap/Taz activation and UUO nephropathy in mice. Mice were performed with UUO and sacrificed at day 7 after surgery. *A* and *B*, Western blot assay (*A*) and quantitative analysis (*B*) showing FN, α-SMA, Yap, and Taz protein abundance in the Sham and UUO kidneys from Gli1^{+}-Rictor$^{+/+}$ and Gli1^{+}-Rictor$^{-/-}$ mice, respectively. *Numbers* indicate individual animals within each group. *, $p < 0.05$ compared with Gli1^{+}-Rictor$^{+/+}$ littermates after UUO ($n = 4$). *C*, representative images showing the lesser induction of Yap/Taz protein in the kidney myofibroblasts from the Gli1^{+}-Rictor$^{-/-}$ mice. *White arrows*, Yap/Taz-positive myofibroblasts. *Scale bar*, 20 μm. *D*, real-time PCR analysis showing the mRNA abundance for *Yap*, *Taz*, *CTGF*, *ANKRD1*, and *TEAD1–4* from Sham and UUO kidneys. *, $p < 0.05$ *versus* Sham control ($n = 5–6$); #, $p < 0.05$ *versus* Rictor$^{+/+}$ littermates after UUO ($n = 5–6$). *E*, representative images of periodic acid–Schiff (*PAS*), Masson, and Sirius red staining in the kidneys from different groups as indicated. *Scale bar*, 20 μm. *F* and *G*, graphic presentation showing the fibrotic area and total collagen content in kidney tissues among groups as indicated. *, $p < 0.05$ compared with Sham control ($n = 4–5$); #, $p < 0.05$ compared with UUO kidneys from control littermates ($n = 4–5$). *Error bars*, S.E.

UUO nephropathy. PP242 was administered (20 mg/kg·day) intraperitoneally from day 2 before to days 7 and 14 after UUO in male CD1 mice. In the UUO kidneys, the protein abundance for p-Akt (Ser-473) and Yap/Taz was largely reduced in mice with PP242 administration compared with the vehicle control (Fig. 5, *A* and *B*). The mRNA abundance of *Yap*/*Taz*, *CTGF*, *ANKRD1*, and *TEAD1–4* was also reduced in the UUO kidneys after PP242 administration compared with those treated with vehicle alone (Fig. 5*C*). Immunofluorescent staining revealed that PP242 could markedly reduce Yap/Taz induction in the myofibroblasts from the fibrotic kidneys (Fig. 5*D*). These data suggest that suppressing mTORC2 with PP242 could inhibit Yap/Taz activation in myofibroblasts from the UUO kidneys in mice.

We then examined kidney fibrosis in mice after PP242 treatment. The results showed that PP242 could reduce FN and α-SMA protein abundance in the UUO kidneys compared with those treated with vehicle alone (Fig. 6*A*). Immunostaining for FN and α-SMA further confirmed the results of a Western blot assay (Fig. 6*B*). Periodic acid–Schiff, Masson, and Sirius red staining showed that tubule injury as well as interstitial matrix deposition were largely attenuated in mice treated with PP242 (Fig. 6*B*). PP242 could also remarkably decrease fibrotic area and total collagen content in the kidneys at day 14 after UUO (Fig. 6, *C* and *D*).

To evaluate the inflammatory cell accumulation in the UUO kidneys, we stained kidney tissue with anti-Ly6b and anti-F4/80 to identify neutrophil and macrophage, respectively. The

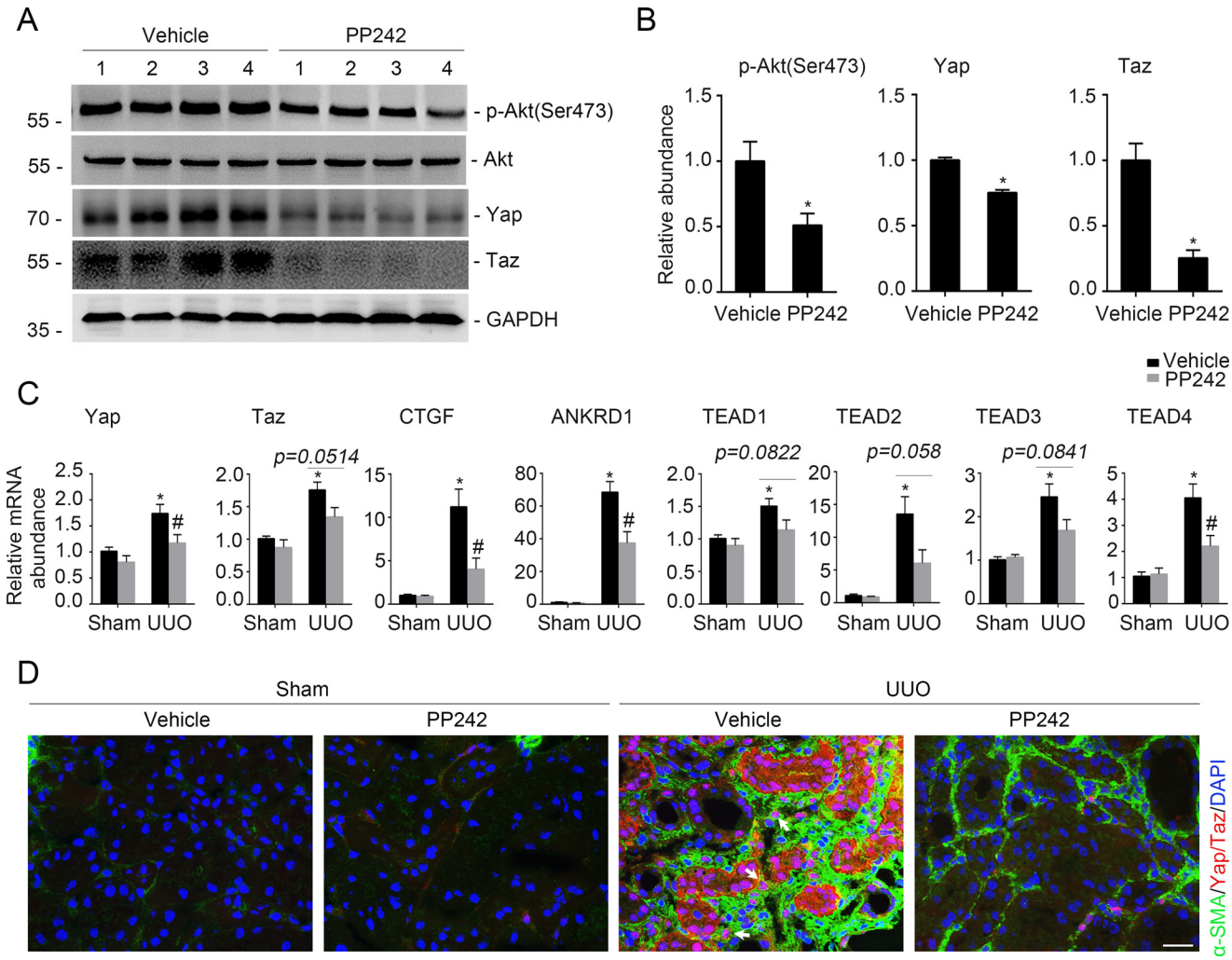

Figure 5. Blockade of mTORC2 signaling with PP242 inactivates Yap/Taz. Male CD1 mice were performed with UUO and sacrificed at day 7 after surgery. *A*, Western blot analysis showing that PP242 administration could inhibit the induction of p-Akt (Ser-473), Yap, and Taz in the fibrotic kidneys with UUO nephropathy compared with those treated with vehicle. The *numbers* indicate the individual animal within each group. *B*, graphic presentation showing the relative abundance for p-Akt (Ser-473), Yap, and Taz, respectively. *, $p < 0.05$ compared with vehicle controls ($n = 4–6$). *C*, real-time PCR analysis showing the mRNA abundance for *Yap*, *Taz*, *CTGF*, *ANKRD1*, and *TEAD1–4* in the kidneys from each group. *, $p < 0.05$ compared with sham control ($n = 5–6$); #, $p < 0.05$ compared with mice treated with vehicle alone ($n = 4–6$). *D*, representative images showing the lesser induction of Yap/Taz protein in the kidney myofibroblasts from the mice treated with PP242 compared with those treated with vehicle. *White arrows*, Yap/Taz-positive myofibroblasts. *Scale bar*, 20 μm. *Error bars*, S.E.

results showed that neutrophil as well as macrophage accumulation was increased in the UUO kidneys from mice treated with vehicle alone, and their accumulation was much lower in PP242-treated UUO kidneys (Fig. 6, *B*, *E*, and *F*). Therefore, it may be concluded that PP242 could inactivate Yap/Taz and ameliorate UUO nephropathy in mice.

Discussion

It has been reported that the mTORC2 pathway is important for promoting the fibrosis process (24, 31–33). In addition, Yap/Taz is the mechano-transducer that regulates TGFβ1 signaling and renal fibrogenesis (15, 16, 27, 34). In this study, we demonstrated that Yap/Taz is a critical mediator for Rictor/mTORC2 in stimulating fibroblast activation and kidney fibrosis based on several lines of evidence. First, both mTORC2 and Yap/Taz were activated in the TGFβ1-stimulated kidney fibroblasts and myofibroblasts from the UUO kidneys. Second, ablation of *Rictor* in fibroblasts/pericytes or pharmacological inhibition of mTORC2 signaling could attenuate Yap/Taz activation and ameliorate kidney fibroblast activation and obstructive nephropathy in mice. Third, overexpression of constitutively active Taz could restore fibroblast activation, which was suppressed by mTORC2 signaling inhibition. To the best of our knowledge, this is the first report that demonstrates the crucial role of Yap/Taz activation in mediating Rictor/mTORC2-promoted kidney fibroblast activation and kidney fibrosis.

The mTOR and Hippo pathways are two major signaling cascades that coordinately regulate cell growth and proliferation (35). Substantial evidence has demonstrated that cross-talk exists between them (25, 26, 36, 37). Artinian *et al.* (26) found that mTORC2 phosphorylating AMOTL2 at Ser-760 results in the blockade of its YAP-binding properties and induces the up-regulation of Yap target genes. MTORC2 may also phosphorylate MST1 at Ser-438 and reduce its dimerization and activity, thereby reducing the phosphorylation of Yap and lead-

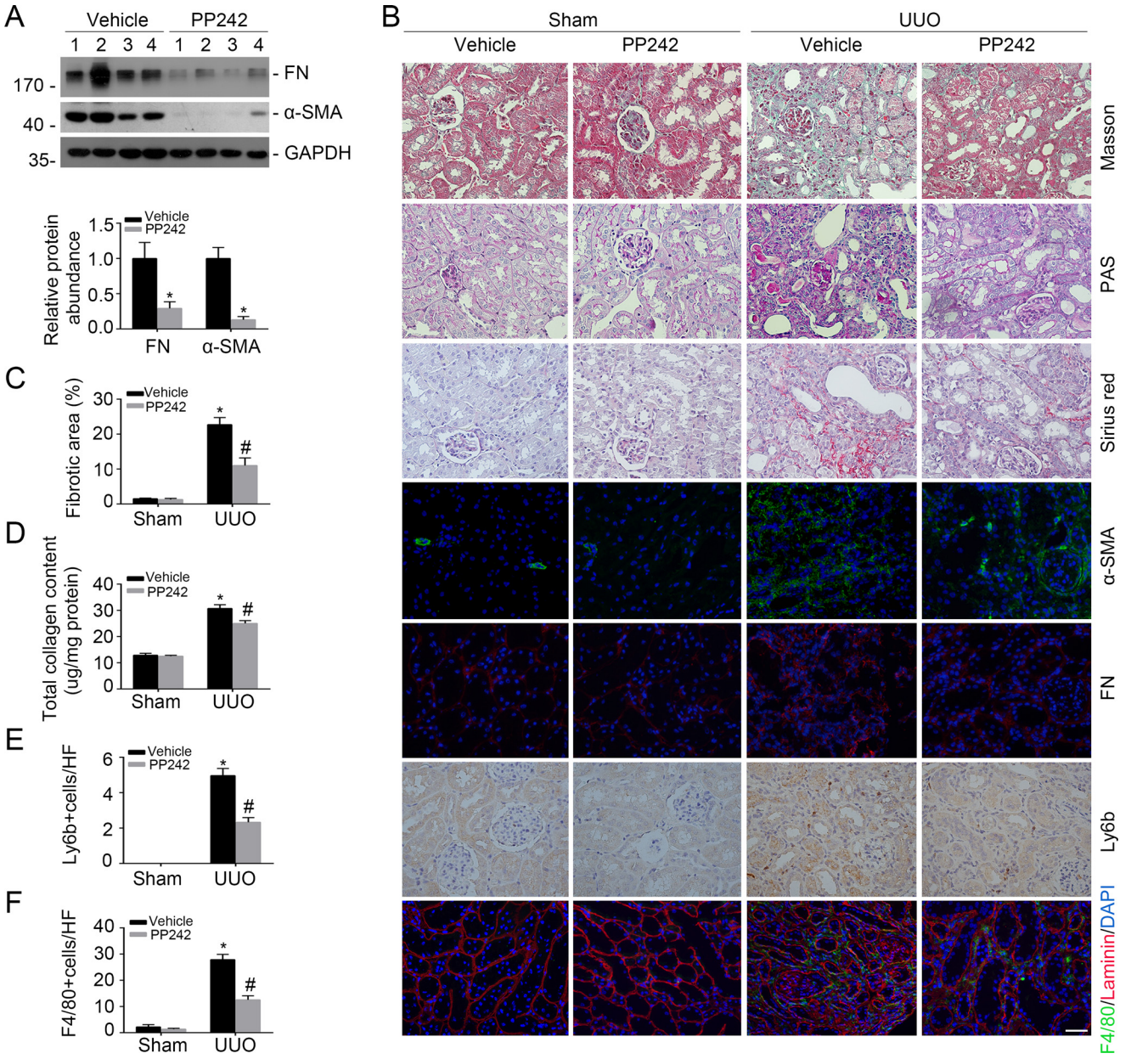

Figure 6. Blockade of mTORC2 signaling with PP242 attenuates UUO nephropathy in mice. Male CD1 mice were performed with UUO and sacrificed at day 14 after surgery. *A*, Western blot analysis showing FN and α-SMA protein abundance in the UUO kidneys from mice treated with vehicle and PP242, respectively. *Numbers* indicate individual animals within each group (*top*). Graphic presentation showing the protein abundance for FN and α-SMA in the UUO kidneys (*bottom*). *, $p < 0.05$ compared with vehicle group ($n = 4$). *B*, representative micrographs showing Masson, periodic acid–Schiff (*PAS*), and Sirius red staining, as well as immunostaining for FN, α-SMA, Ly6b, and F4/80 in the contralateral (*CTL*) and UUO kidneys from various groups as indicated. *Scale bar*, 20 μm. *C–F*, graphic presentation showing the fibrotic area (*C*), total collagen content (*D*), neutrophils (*E*), and macrophages (*F*) in kidney tissues among groups as indicated. *, $p < 0.05$ compared with CTL kidneys ($n = 3–6$); #, $p < 0.05$ compared with UUO kidneys with vehicle ($n = 3–6$). *Error bars*, S.E.

ing to Yap activation (25). Additionally, mTOR has been reported to be able to up-regulate Yap expression through impairing the autophagy-induced Yap degradation (36). Yap could regulate the mTOR pathway via miR-29 (37). Studies have disclosed that activated LATS1/2 could phosphorylate Yap/Taz, thereby inducing their cytoplasmic sequestration and inactivation (7, 38–40). In this study, we demonstrated that TGFβ1 could up-regulate Yap/Taz expression through mTORC2 signaling-stimulated Yap/Taz transcriptional activation. This conclusion is supported by the following evidence: 1) TGFβ1 could markedly up-regulate the protein and mRNA expression of Yap/Taz in cultured kidney fibroblasts, which were largely suppressed by PP242 or Akt1/2 inhibitor; 2) in the fibrotic kidneys with UUO nephropathy, the mRNA and protein abundance of Yap/Taz and TEAD1–4 were increased, and these were largely suppressed in the mice with fibroblast ablation of *Rictor* or treated with PP242; 3) blocking gene transcription and translation with actinomycin D and cycloheximide, respectively, could almost completely abolish TGFβ1-induced Yap/Taz up-regulation. However, the molecular mechanisms for Rictor/mTORC2 signaling in stimulating the Yap/Taz transcription remain to be further clarified.

Fibroblasts/pericytes play an essential role in kidney ECM deposition and renal fibrosis upon activation (41–43). Our pre-

vious study reported that ablation of *Rictor* in fibroblasts could attenuate UUO nephropathy in mice (24). In that study, S100A4-Cre transgenic mice were employed to generate the mice with fibroblast ablation of the *Rictor*. Recently, studies have demonstrated that Gli1 marks a perivascular mesenchymal stem cell–like progenitor population (28, 44). In kidneys with UUO nephropathy, resident Gli1$^+$ cells are able to be transformed to myofibroblasts and promote kidney fibrosis (28, 44, 46). In this study, we generated a mice model with Gli1$^+$-fibroblast/pericyte ablation of *Rictor* by cross-breeding Rictor-floxed mice with the Gli1-CreERT2 transgenic mice, in which Cre recombinase expression is under the control of the endogenous Gli1 promoter (46). Compared with the S100A4-Cre transgenic mice, Gli1-CreERT2 transgenic mice provide an alternative option that deletes the target genes in fibroblasts/pericytes. Additionally, Cre recombinase expression in Gli1-CreERT2 transgenic mice is tamoxifen-inducible, which may facilitate the investigation for the pathogenic role of target genes under diseased conditions. Consistent with our previous report using S100A4-Cre transgenic mice (24), kidney fibrosis was attenuated in the UUO kidneys from the mice with Gli1$^+$-fibroblast/pericyte ablation of *Rictor*. It should be noted that only part of the fibroblasts within the kidneys express Gli1, so the effects of Rictor/mTORC2 signaling in promoting fibroblast activation and kidney fibrosis may be underscored by using this model. Nevertheless, based on the results from two different mouse models with fibroblast ablation of *Rictor*, it is concluded that Rictor/mTORC2 signaling activation plays a crucial role in promoting fibroblast activation and kidney fibrosis. This conclusion was further supported by the pharmacologic inhibition of mTORC2 signaling with PP242, in which kidney fibrosis induced after UUO operation was largely ameliorated. It should be noted that Yap/Taz was also activated in tubular epithelial cells after UUO, suggesting a potential role for epithelial Hippo pathway in kidney fibrosis.

In summary, our study demonstrated that Yap/Taz is indispensable for Rictor/mTORC2-stimulated kidney fibrogenic process. Blockade of mTORC2/Yap/Taz may shed new light on attenuating kidney fibrosis for patients with chronic kidney disease.

Experimental procedures

Mice and animal models

Homozygous Rictor-floxed mice (C57BL/6J background) were kindly provided by Dr. Magnuson (Vanderbilt University). By mating Rictor-floxed mice (C57BL/6J background) with Gli1-CreERT2 transgenic mice (007913, C57BL/6J background, Jackson Laboratory, Bar Harbor, ME) (46), mice that were heterozygous for the Rictor-floxed allele were generated (genotype: Rictor$^{fl/wt}$, Cre$^{+/-}$). These mice were cross-bred with homozygous Rictor-floxed mice (genotype: Rictor$^{fl/fl}$) to generate offspring with genotyping Rictor$^{fl/fl}$, Cre$^{+/-}$. The breeding protocol also generated mice with genotyping Rictor$^{fl/fl}$, Cre$^{-/-}$, which from the same litters with the knockouts were considered as control littermates. Genotyping was performed by a PCR assay using DNA extracted from the mouse tail. The primers used for genotyping were as follows: Cre transgene, 5′-TTGCCTGCATTACCGGTCGATGC-3′ (sense) and 5′-TTGCACGTTCACCGGCATCAACG-3′ (antisense); Rictor genotyping, 5′-GACACTGGATTACAGTGGCTTG-3′ (sense) and 5′-GCTGGGCCATCTGAATAACTTC-3′ (antisense). To induce specific deletion of Rictor in fibroblasts, mice with genotyping Gli1-Cre$^{+/-}$, Rictor$^{fl/fl}$ were intraperitoneally injected with tamoxifen (T5648, Sigma-Aldrich) at 25 mg/kg for 5 consecutive days. The control littermates were also injected with tamoxifen. Two days after the last injection, mice were subjected to UUO surgery.

Male CD-1 mice weighing ~18–20 g were acquired from the specific pathogen-free Laboratory Animal Center of Nanjing Medical University, and we performed UUO experiments on these as reported previously (47). The animals were divided into two groups; mice were 1) injected with vehicle or 2) treated with PP242 (20 mg/kg·day) from 2 days before to 1 or 2 weeks after surgery. PP242 (catalog no. S221, Selleckchem) was prepared in a 10% DMSO solution and injected intraperitoneally. The mice were euthanized on days 7 and 14 after UUO. The UUO kidneys as well as the contralateral kidneys were removed. One portion of the kidney was fixed in 10% phosphate-buffered formalin, followed by paraffin embedding for histological and immunohistochemical staining. Another portion was immediately frozen in Tissue-Tek optimum cutting temperature compound (Sakura Finetek, Torrance, CA) for cryosection. The remaining kidney tissue was snap-frozen in liquid nitrogen and stored at −80 °C for extraction of RNA and protein.

All animals were maintained in the specific pathogen-free Laboratory Animal Center of Nanjing Medical University according to the guidelines of the institutional animal care and use committee at Nanjing Medical University (Nanjing, China). All experiments were performed in accordance with the approved guidelines and regulations of the Animal Experimentation Ethics Committee at Nanjing Medical University. The work described has been carried out in accordance with EU Directive 2010/63/EU for animal experiments.

Cell culture and treatment

NRK-49F cells were obtained from American Type Culture Collection (Manassas, VA). Cells were cultured in Dulbecco's modified Eagle's medium/F-12 medium supplemented with 5% newborn calf serum (Gibco). The cells were seeded on 6-well culture plates to 60–70% confluence in complete medium containing 5% newborn calf serum for 16 h and then changed to serum-free medium after washing twice with serum-free medium. To generate kidney fibroblasts with *Rictor* gene deletion, primary cultured kidney fibroblasts from Gli1-Cre$^{+/-}$, Rictor$^{fl/fl}$ mice were generated from kidney cortex and infected with adenovirus carrying Cre recombinase. Recombinant human TGFβ1 (catalog no. 100-B-010-CF, R&D Systems, Minneapolis, MN) was added to the serum-free medium for various durations. PP242 (catalog no. P0037, Sigma-Aldrich) was added at concentrations of 3.2, 16, 80, and 400 nM. Rapamycin (1.28 nM) (catalog no. R8781, Sigma-Aldrich) was added at 30 min before TGFβ1 stimulation. Cells were treated with verteporfin (catalog no. SML0534, Sigma-Aldrich), Akt1/2 kinase inhibitor

(catalog no. A6730, Sigma-Aldrich), CHX (Beyotime, Shanghai, China), and actinomycin D (Sigma-Aldrich) for the indicated durations. Yap, Taz, or scramble siRNA (GenePharma, Shanghai, China) and 3×FLAG pCMV5-TOPO-TAZ (S89A) plasmid were transfected into NRK-49F cells using Lipofectamine 2000 reagent (Invitrogen) according to the manufacturer's instructions. 3×FLAG pCMV5-TOPO TAZ (S89A) was a gift from Jeff Wrana (Addgene plasmid 24815).

Histology and immunohistochemistry

Kidney samples were fixed in 10% neutral formalin and embedded in paraffin. Sections at 3-μm thickness were stained with periodic acid–Schiff, Masson, and Sirius red. For immunohistochemical staining, paraffin-embedded kidney sections were deparaffinized, hydrated, and antigen-retrieved. Endogenous peroxidase activity was quenched by 3% H_2O_2. Sections were then blocked with 10% normal donkey serum, followed by incubation with anti-Ly6b (catalog no. 0715, Bio-Rad) overnight at 4 °C. After incubation with secondary antibody for 1 h, sections were incubated with ABC reagents for 1 h at room temperature before being subjected to substrate 3-amino-9-ethylcarbazole or 3,3′-diaminobenzidine (Vector Laboratories, Burlingame, CA). Slides were viewed with a Nikon Eclipse 80i microscope equipped with a digital camera (DS-Ri1, Nikon, Shanghai, China).

Immunofluorescent staining

Kidney cryosections at 3-μm thickness were fixed for 15 min in 4% paraformaldehyde, followed by permeabilization with 0.2% Triton X-100 in PBS for 5 min at room temperature. After blocking with 2% donkey serum for 60 min, the slides were immunostained with anti-FN (catalog no. F3648, Sigma -Aldrich), anti-α-SMA (catalog no. A5228, Sigma-Aldrich), anti-F4/80 (catalog no. 14-4801, eBioscience, San Diego, CA), anti-p-Akt (Ser-473) (catalog no. 3868, Cell Signaling Technology, Shanghai, China), anti-TEAD (D3F7L) (catalog no. 13295, Cell Signaling Technology), or anti-Yap/Taz (D24E4) (catalog no. 8418S, Cell Signaling Technology). NRK-49F cells cultured on coverslips were washed twice with cold 1× PBS and fixed with cold methanol/acetone (1:1) for 10 min at −20 °C. After three extensive washings with 1× PBS, the cells were treated with 0.1% Triton X-100 for 5 min and blocked with 2% normal donkey serum in 1× PBS buffer for 40 min at room temperature and incubated with the anti-FN or anti-α-SMA, followed by staining with FITC or tetramethylrhodamine-conjugated secondary antibody. Cells were also stained with 4′,6-diamidino-2-phenylindole to visualize the nuclei. Slides were viewed with a Nikon Eclipse 80i epifluorescence microscope equipped with a digital camera.

Western blot analysis

NRK-49F cells and primary cultured kidney fibroblasts were lysed in 1× SDS sample buffer. The kidney tissues were lysed with radioimmunoprecipitation assay solution containing 1% Nonidet P-40, 0.1% SDS, 100 μg/ml phenylmethylsulfonyl fluoride, 1% protease inhibitor mixture, and 1% phosphatase I and II inhibitor mixture (Sigma) on ice. The supernatants were collected after centrifugation at 13,000 × g at 4 °C for 30 min. Protein concentration was determined by a bicinchoninic acid protein assay (BCA kit; Pierce) according to the manufacturer's instructions. An equal amount of protein was loaded onto SDS-PAGE and transferred onto polyvinylidene difluoride membranes. The primary antibodies were as follows: anti-GAPDH (catalog no. FL-335, Santa Cruz Biotechnology, Inc., Dallas, TX), anti-p-Akt (Ser-473) (catalog no. 3868, Cell Signaling Technology), anti-FN (catalog no. F3648, Sigma-Aldrich), anti-α-SMA (catalog no. A5228, Sigma-Aldrich), anti-TEAD (D3F7L) (catalog no. 13295, Cell Signaling Technology), anti-Yap/Taz (D24E4) (catalog no. 8418, Cell Signaling Technology), and anti-Yap (catalog no. 4912S, Cell Signaling Technology). Quantification was performed by measuring the intensity of the signals with the aid of the National Institutes of Health ImageJ software package.

RNA isolation and real-time quantitative reverse transcription-PCR

Total RNA was extracted using TRIzol reagent (Invitrogen) according to the manufacturer's instructions. cDNA was synthesized with 1 μg of total RNA, ReverTra Ace (Vazyme, Nanjing, China), and oligo(dT) 12–18 primers. Gene expression was measured by real-time PCR assay (Vazyme) and a 7300 real-time PCR system (Applied Biosystems, Foster City, CA). The amount of mRNA or gene relative to internal control was calculated using the equation, $2\Delta CT$, in which $\Delta CT = CT_{\text{gene}} - CT_{\text{control}}$.

Statistical analysis

All data examined are presented as mean ± S.E. Statistical analysis of the data was performed using the SigmaStat software (Jandel Scientific Software, San Rafael, CA). Comparison between groups was made using one-way analysis of variance, followed by the Student-Newman-Keuls test. $p < 0.05$ was considered as statistically significant.

Author contributions—Y. G., J. L., Q. L., Y. F., and M. W. performed the experiments. Y. G. wrote the manuscript. J. Y. and W. H. analyzed the data. C. D. designed and supervised the study and revised the manuscript.

References

1. Liu, Y. (2011) Cellular and molecular mechanism of renal fibrosis. *Nat. Rev. Nephrol.* **7,** 684–696 CrossRef Medline
2. Meguid El Nahas, A., and Bello, A. K. (2005) Chronic kidney disease: the global challenge. *Lancet* **365,** 331–340 CrossRef Medline
3. Grande, M. T., and López-Novoa, J. M. (2009) Fibroblast activation and myofibroblast generation in obstructive nephropathy. *Nat. Rev. Nephrol.* **5,** 319–328 CrossRef Medline
4. Nath, K. A. (1992) Tubulointerstitial changes as a major determinant in the progression of renal damage. *Am. J. Kidney Dis.* **20,** 1–17 CrossRef Medline
5. Humphreys, B. D. (2018) Mechanisms of renal fibrosis. *Annu. Rev. Physiol.* **80,** 309–326 CrossRef Medline
6. Zhao, B., Tumaneng, K., and Guan, K. L. (2011) The Hippo pathway in organ size control, tissue regeneration and stem cell self-renewal. *Nat. Cell Biol.* **13,** 877–883 CrossRef Medline
7. Lei, Q. Y., Zhang, H., Zhao, B., Zha, Z. Y., Bai, F., Pei, X. H., Zhao, S., Xiong, Y., and Guan, K. L. (2008) TAZ promotes cell proliferation and epithelial-

mesenchymal transition and is inhibited by the hippo pathway. *Mol. Cell. Biol.* **28,** 2426–2436 CrossRef Medline
8. Hong, A. W., Meng, Z., and Guan, K. L. (2016) The Hippo pathway in intestinal regeneration and disease. *Nat. Rev. Gastroenterol. Hepatol.* **13,** 324–337 CrossRef Medline
9. Yagi, R., Chen, L. F., Shigesada, K., Murakami, Y., and Ito, Y. (1999) A WW domain-containing Yes-associated protein (YAP) is a novel transcriptional co-activator. *EMBO J.* **18,** 2551–2562 CrossRef Medline
10. Zhang, L., Ren, F., Zhang, Q., Chen, Y., Wang, B., and Jiang, J. (2008) The TEAD/TEF family of transcription factor scalloped mediates Hippo signaling in organ size control. *Dev. Cell* **14,** 377–387 CrossRef Medline
11. Komuro, A., Nagai, M., Navin, N. E., and Sudol, M. (2003) WW domain-containing protein YAP associates with ErbB-4 and acts as a co-transcriptional activator for the carboxyl-terminal fragment of ErbB-4 that translocates to the nucleus. *J. Biol. Chem.* **278,** 33334–33341 CrossRef Medline
12. Dupont, S., Morsut, L., Aragona, M., Enzo, E., Giulitti, S., Cordenonsi, M., Zanconato, F., Le Digabel, J., Forcato, M., Bicciato, S., Elvassore, N., and Piccolo, S. (2011) Role of YAP/TAZ in mechanotransduction. *Nature* **474,** 179–183 CrossRef Medline
13. Aragona, M., Panciera, T., Manfrin, A., Giulitti, S., Michielin, F., Elvassore, N., Dupont, S., and Piccolo, S. (2013) A mechanical checkpoint controls multicellular growth through YAP/TAZ regulation by actin-processing factors. *Cell* **154,** 1047–1059 CrossRef Medline
14. Chen, J., and Harris, R. C. (2016) Interaction of the EGF receptor and the Hippo pathway in the diabetic kidney. *J. Am. Soc. Nephrol.* **27,** 1689–1700 CrossRef Medline
15. Szeto, S. G., Narimatsu, M., Lu, M., He, X., Sidiqi, A. M., Tolosa, M. F., Chan, L., De Freitas, K., Bialik, J. F., Majumder, S., Boo, S., Hinz, B., Dan, Q., Advani, A., John, R., *et al.* (2016) YAP/TAZ are mechanoregulators of TGF-β-Smad signaling and renal fibrogenesis. *J. Am. Soc. Nephrol.* **27,** 3117–3128 CrossRef Medline
16. Liang, M., Yu, M., Xia, R., Song, K., Wang, J., Luo, J., Chen, G., and Cheng, J. (2017) Yap/Taz deletion in Gli+ cell-derived myofibroblasts attenuates fibrosis. *J. Am. Soc. Nephrol.* **28,** 3278–3290 CrossRef Medline
17. Johnson, S. C., Rabinovitch, P. S., and Kaeberlein, M. (2013) mTOR is a key modulator of ageing and age-related disease. *Nature* **493,** 338–345 CrossRef Medline
18. Stanfel, M. N., Shamieh, L. S., Kaeberlein, M., and Kennedy, B. K. (2009) The TOR pathway comes of age. *Biochim. Biophys. Acta* **1790,** 1067–1074 CrossRef Medline
19. Cybulski, N., and Hall, M. N. (2009) TOR complex 2: a signaling pathway of its own. *Trends Biochem. Sci.* **34,** 620–627 CrossRef Medline
20. Goncharova, E. A., Goncharov, D. A., Li, H., Pimtong, W., Lu, S., Khavin, I., and Krymskaya, V. P. (2011) mTORC2 is required for proliferation and survival of TSC2-null cells. *Mol. Cell. Biol.* **31,** 2484–2498 CrossRef Medline
21. Kocalis, H. E., Hagan, S. L., George, L., Turney, M. K., Siuta, M. A., Laryea, G. N., Morris, L. C., Muglia, L. J., Printz, R. L., Stanwood, G. D., Niswender, K. D. (2014) Rictor/mTORC2 facilitates central regulation of energy and glucose homeostasis. *Mol. Metab.* **3,** 394–407 CrossRef Medline
22. Laplante, M., and Sabatini, D. M. (2009) mTOR signaling at a glance. *J. Cell Sci.* **122,** 3589–3594 CrossRef Medline
23. Sarbassov, D. D., Ali, S. M., Kim, D. H., Guertin, D. A., Latek, R. R., Erdjument-Bromage, H., Tempst, P., and Sabatini, D. M. (2004) Rictor, a novel binding partner of mTOR, defines a rapamycin-insensitive and raptor-independent pathway that regulates the cytoskeleton. *Curr. Biol.* **14,** 1296–1302 CrossRef Medline
24. Li, J., Ren, J., Liu, X., Jiang, L., He, W., Yuan, W., Yang, J., and Dai, C. (2015) Rictor/mTORC2 signaling mediates TGFβ1-induced fibroblast activation and kidney fibrosis. *Kidney Int.* **88,** 515–527 CrossRef Medline
25. Sciarretta, S., Zhai, P., Maejima, Y., Del Re, D. P., Nagarajan, N., Yee, D., Liu, T., Magnuson, M. A., Volpe, M., Frati, G., Li, H., and Sadoshima, J. (2015) mTORC2 regulates cardiac response to stress by inhibiting MST1. *Cell Rep.* **11,** 125–136 CrossRef Medline
26. Artinian, N., Cloninger, C., Holmes, B., Benavides-Serrato, A., Bashir, T., and Gera, J. (2015) Phosphorylation of the Hippo pathway component AMOTL2 by the mTORC2 kinase promotes YAP signaling, resulting in enhanced glioblastoma growth and invasiveness. *J. Biol. Chem.* **290,** 19387–19401 CrossRef Medline
27. Varelas, X., Sakuma, R., Samavarchi-Tehrani, P., Peerani, R., Rao, B. M., Dembowy, J., Yaffe, M. B., Zandstra, P. W., and Wrana, J. L. (2008) TAZ controls Smad nucleocytoplasmic shuttling and regulates human embryonic stem-cell self-renewal. *Nat. Cell Biol.* **10,** 837–848 CrossRef Medline
28. Kramann, R., Wongboonsin, J., Chang-Panesso, M., Machado, F. G., and Humphreys, B. D. (2017) Gli1$^+$ pericyte loss induces capillary rarefaction and proximal tubular injury. *J. Am. Soc. Nephrol.* **28,** 776–784 Medline
29. Chen, Y. T., Chang, F. C., Wu, C. F., Chou, Y. H., Hsu, H. L., Chiang, W. C., Shen, J., Chen, Y. M., Wu, K. D., Tsai, T. J., Duffield, J. S., and Lin, S. L. (2011) Platelet-derived growth factor receptor signaling activates pericyte-myofibroblast transition in obstructive and post-ischemic kidney fibrosis. *Kidney Int.* **80,** 1170–1181 CrossRef Medline
30. Lin, S. L., Kisseleva, T., Brenner, D. A., and Duffield, J. S. (2008) Pericytes and perivascular fibroblasts are the primary source of collagen-producing cells in obstructive fibrosis of the kidney. *Am. J. Pathol.* **173,** 1617–1627 CrossRef Medline
31. Ren, J., Li, J., Feng, Y., Shu, B., Gui, Y., Wei, W., He, W., Yang, J., and Dai, C. (2017) Rictor/mTORC2 promotes macrophage activation and kidney fibrosis. *J. Pathol.* **242,** 488–499 CrossRef Medline
32. Lamouille, S., Connolly, E., Smyth, J. W., Akhurst, R. J., and Derynck, R. (2012) TGF-β-induced activation of mTOR complex 2 drives epithelial-mesenchymal transition and cell invasion. *J. Cell Sci.* **125,** 1259–1273 CrossRef Medline
33. Serrano, I., McDonald, P. C., Lock, F. E., and Dedhar, S. (2013) Role of the integrin-linked kinase (ILK)/Rictor complex in TGFβ-1-induced epithelial-mesenchymal transition (EMT). *Oncogene* **32,** 50–60 CrossRef Medline
34. Piersma, B., de Rond, S., Werker, P. M., Boo, S., Hinz, B., van Beuge, M. M., and Bank, R. A. (2015) YAP1 is a driver of myofibroblast differentiation in normal and diseased fibroblasts. *Am. J. Pathol.* **185,** 3326–3337 CrossRef Medline
35. Csibi, A., and Blenis, J. (2012) Hippo-YAP and mTOR pathways collaborate to regulate organ size. *Nat. Cell Biol.* **14,** 1244–1245 CrossRef Medline
36. Liang, N., Zhang, C., Dill, P., Panasyuk, G., Pion, D., Koka, V., Gallazzini, M., Olson, E. N., Lam, H., Henske, E. P., Dong, Z., Apte, U., Pallet, N., Johnson, R. L., Terzi, F., *et al.* (2014) Regulation of YAP by mTOR and autophagy reveals a therapeutic target of tuberous sclerosis complex. *J. Exp. Med.* **211,** 2249–2263 CrossRef Medline
37. Tumaneng, K., Schlegelmilch, K., Russell, R. C., Yimlamai, D., Basnet, H., Mahadevan, N., Fitamant, J., Bardeesy, N., Camargo, F. D., and Guan, K. L. (2012) YAP mediates crosstalk between the Hippo and PI3K-TOR pathways by suppressing PTEN via miR-29. *Nat. Cell Biol.* **14,** 1322–1329 CrossRef Medline
38. Zhao, B., Wei, X., Li, W., Udan, R. S., Yang, Q., Kim, J., Xie, J., Ikenoue, T., Yu, J., Li, L., Zheng, P., Ye, K., Chinnaiyan, A., Halder, G., Lai, Z. C., Guan, K. L. (2007) Inactivation of YAP oncoprotein by the Hippo pathway is involved in cell contact inhibition and tissue growth control. *Genes Dev.* **21,** 2747–2761 CrossRef Medline
39. Hao, Y., Chun, A., Cheung, K., Rashidi, B., and Yang, X. (2008) Tumor suppressor LATS1 is a negative regulator of oncogene YAP. *J. Biol. Chem.* **283,** 5496–5509 CrossRef Medline
40. Zhao, B., Li, L., Tumaneng, K., Wang, C. Y., and Guan, K. L. (2010) A coordinated phosphorylation by Lats and CK1 regulates YAP stability through SCFβ-TRCP. *Genes Dev.* **24,** 72–85 CrossRef Medline
41. Duffield, J. S., and Humphreys, B. D. (2011) Origin of new cells in the adult kidney: results from genetic labeling techniques. *Kidney Int.* **79,** 494–501 CrossRef Medline
42. Eddy, A. A. (1996) Molecular insights into renal interstitial fibrosis. *J. Am. Soc. Nephrol.* **7,** 2495–2508 Medline
43. Quaggin, S. E., and Kapus, A. (2011) Scar wars: mapping the fate of epithelial-mesenchymal-myofibroblast transition. *Kidney Int.* **80,** 41–50 CrossRef Medline
44. Kramann, R., Schneider, R. K., DiRocco, D. P., Machado, F., Fleig, S., Bondzie, P. A., Henderson, J. M., Ebert, B. L., and Humphreys, B. D. (2015)

Perivascular Gli1$^+$ progenitors are key contributors to injury-induced organ fibrosis. *Cell Stem Cell* **16,** 51–66 CrossRef Medline

45. Kramann, R., Fleig, S. V., Schneider, R. K., Fabian, S. L., DiRocco, D. P., Maarouf, O., Wongboonsin, J., Ikeda, Y., Heckl, D., Chang, S. L., Rennke, H. G., Waikar, S. S., and Humphreys, B. D. (2015) Pharmacological GLI2 inhibition prevents myofibroblast cell-cycle progression and reduces kidney fibrosis. *J. Clin. Invest.* **125,** 2935–2951 CrossRef Medline
46. Ahn, S., and Joyner, A. L. (2004) Dynamic changes in the response of cells to positive hedgehog signaling during mouse limb patterning. *Cell* **118,** 505–516 CrossRef Medline
47. Feng, Y., Ren, J., Gui, Y., Wei, W., Shu, B., Lu, Q., Xue, X., Sun, X., He, W., Yang, J., and Dai, C. (2018) Wnt/β-catenin-promoted macrophage alternative activation contributes to kidney fibrosis. *J. Am. Soc. Nephrol.* **29,** 182–193 CrossRef Medline